# A SURVEY OF YOUNG STARS IN THE TAURUS MOLECULAR CLOUD WITH XMM-NEWTON

**M. Güdel, K. Briggs, A. Telleschi, K. Arzner[1], M. Audard[2], N. Grosso, J. Bouvier[3], E. Franciosini, G. Micela, I. Pillitteri, L. Scelsi, B. Stelzer[4], F. Palla[5], and D. Padgett, L. Rebull[6]**

[1]Paul Scherrer Institut, Würenlingen and Villigen, CH-5232 Villigen PSI
[2]Columbia University, New York, NY 10027, USA
[3]LAOG, Université J. Fourier, F-38041 Grenoble
[4]Osservatorio Astronomico di Palermo, I-90134 Palermo
[5]Osservatorio Astrofisico di Arcetri, I-50125 Firenze
[6]Spitzer Science Center, Caltech, Pasadena, CA, USA

## ABSTRACT

The Taurus Molecular Cloud (TMC) ranks among the nearest and best-studied low-mass star formation regions. We have initiated comprehensive surveys of the TMC, in particular including a deep X-ray survey of nearly 5 sq. degrees with *XMM-Newton* and a near-to-mid-infrared photometric survey of 29 sq. degrees with the Spitzer Space Telescope, mapping the entire cloud in all available photometric bands. We present a summary of selected aspects of the X-ray results in the context of the TMC population and evolution. We address the physical interpretation of our new X-ray data and discuss the young stellar population.

Key words: Taurus Molecular Cloud, X-rays.

## 1. INTRODUCTION

In a modern picture of star formation, complex feedback loops regulate mass accretion processes, the ejection of jets and outflows, and the chemical and physical evolution of disk material destined to form planets. Observations in X-rays with *Chandra* and *XMM-Newton* penetrate dense molecular envelopes, revealing an environment exposed to high levels of hard X-ray radiation.

X-rays play a crucial role in studies of star formation, both physically and diagnostically. They may be generated at various locations in young stellar systems, such as in a "solar-like" coronal/magnetospheric environment, in shocks forming in accretion funnel flows or in jets and Herbig-Haro flows. But it remains unclear to what extent accretion-related phenomena influence X-ray production.

The Taurus Molecular Cloud (TMC henceforth) has played a fundamental role in our understanding of low-mass star formation. At a distance around 140 pc (van den Ancker et al., 1997), it is one of the nearest star formation regions (SFR) and reveals characteristics that make it ideal for detailed physical studies. One of the most notable properties of TMC in this regard is its structure in which several loosely associated but otherwise rather isolated molecular cores each produce one or only a few low-mass stars, different from the much denser cores in $\rho$ Oph or in Orion.

In X-rays, TMC has played a key role in our understanding of high-energy processes and circumstellar magnetic fields around pre-main sequence stars. Among the key surveys are those by Feigelson et al. (1987), Walter et al. (1988), Bouvier (1990), Strom et al. (1990), Damiani et al. (1995) and Damiani & Micela (1995) based on *Einstein Observatory* observations, and the work by Strom & Strom (1994), Neuhäuser et al. (1995) and Stelzer & Neuhäuser (2001) based on *ROSAT*. These surveys have characterized the overall luminosity behavior of TTS, indicated a rotation-activity relation, and partly suggested X-ray differences between CTTS and WTTS.

We have started a large multi-wavelength project to map significant portions of TMC in X-rays (EPIC example in Fig. 1), the optical, and the infrared. Our *XMM-Newton* X-ray survey maps approximately 5 sq. deg of the denser cloud areas with limiting sensitivities around $L_X \approx 10^{28}$ erg s$^{-1}$, sufficient to detect every lightly absorbed, normal CTTS and WTTS in the cloud, and of order 50% of all brown dwarfs (BDs) and protostars.

## 2. DETECTION STATISTICS

The detection statistics of our survey is summarized in Table 1. An important point for further statistical studies is that the X-ray sample of detected CTTS and WTTS is essentially complete for the surveyed fields (as far as the
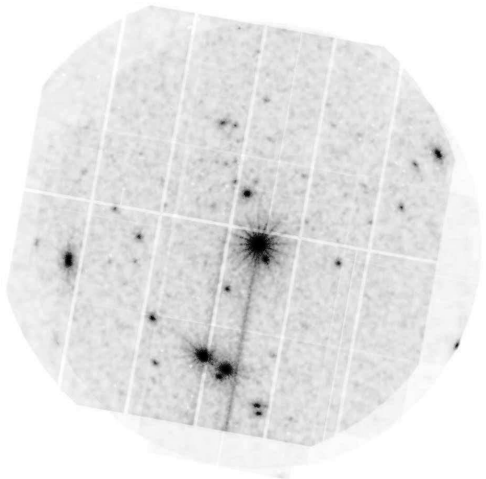
*Figure 1. Example of an EPIC image (the field around V410 Tau = L1495). The field diameter is 30′, and the point-spread function has an FWHM of about 5″.*

population is known). The few remaining, undetected objects are either heavily absorbed, have unclear YSO classification, or are objects that have been very poorly studied before, so that their status as TMC members may be questionable. In contrast, previous X-ray surveys did not detect the intrinsically fainter TTS population, potentially introducing bias into statistical correlations and population studies. It is little surprising that some of the protostars remained undetected given the strong photoelectric absorption. Most of the detected protostars show no X-ray counts below 2 keV. The detection rate of BDs (53%) is also very favorable (Grosso et al., 2006); the remaining objects of this class are likely to be intrinsically fainter than our detection limit rather than being excessively absorbed by gas ($A_V$ of those objects typically being no more than few magnitudes).

## 2.1. X-Ray Luminosity

Fig. 2 shows the distribution of X-ray luminosities $L_X$ as a function of $L_{\rm bol}$ for all spectrally modeled TTS and protostars, and also including the *detected* BDs (we exclude the peculiar sources discussed in Sect. 3 below; some objects were observed twice with different $L_X$ - each result is shown separately in this plot). We do not give errors for $L_X$ because most objects are variable on short and long

*Table 1. X-ray detection statistics*

| Object type | members surveyed | Detections | Detection fraction |
|---|---|---|---|
| Protostars | 18 | 7 | 39% |
| CTTS | 66 | 60 | 91% |
| WTTS | 42 | 39 | 93% |
| Brown Dwarfs | 19 | 10 | 53% |

time scales (hours to days), typically within a factor of two outside obvious, outstanding flares. Most stars cluster between $L_X/L_{\rm bol} = 10^{-4} - 10^{-3}$ as is often found in star-forming regions. The value $L_X/L_{\rm bol} = 10^{-3}$ corresponds to the saturation value for rapidly rotating main-sequence stars (see below). We also note a trend for somewhat higher levels of $L_X/L_{\rm bol}$ for higher $L_{\rm bol}$ (typically, more massive stars). What controls the X-ray luminosity level? Given the trend toward saturation in Fig. 2, one key parameter is obviously $L_{\rm bol}$. Although for pre-main sequence stars there is no strict correlation between $L_{\rm bol}$ and stellar mass, it is interesting that we find a rather well-developed correlation between $L_X$ and mass $M$ (Fig. 3). Part of this correlation might be explained by higher-mass stars being larger, i.e., providing more surface area for coronal active regions. The correlation between surface area and $L_X$ is, however, considerably weaker than the trend shown in Fig. 3, and for constant average stellar density, we would expect $L_X \propto M^{2/3}$ rather than $L_X \propto M^{1.54\pm0.14}$ as found here.
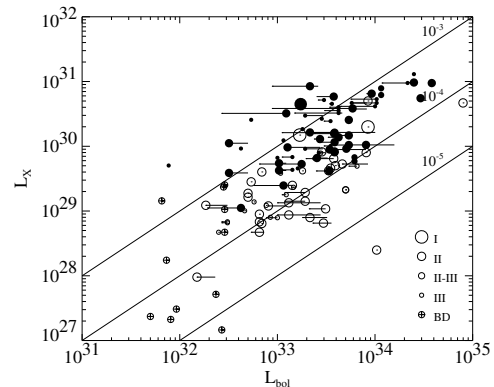


*Figure 2. Plot of $L_X$ vs. $L_{\rm bol}$ for X-ray detected (and spectrally modeled) stars and BDs. The diagonal lines are the loci where $L_X = (10^{-3}, 10^{-4}, 10^{-5})L_{\rm bol}$, respectively. Key to the symbols: Size, from largest to smallest: protostars (Class I) - CTTS (Class II) - Class II-III (uncertain classification) - WTTS (Class III). Circles with crosses: BDs. Filled: $\geq 400$ cts in X-ray spectrum; open circles: $< 400$ cts. The error bars indicate ranges of $L_{\rm bol}$ given in the literature.*
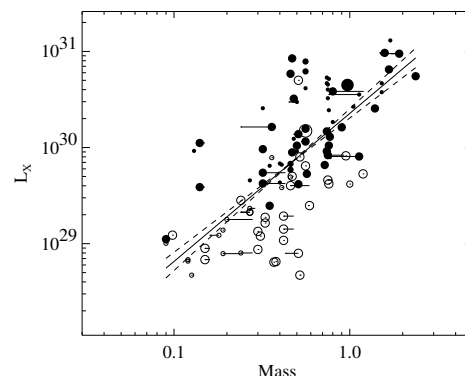


*Figure 3. X-ray luminosity $L_X$ vs. stellar mass. A clear correlation is visible (regression line overplotted). Key to the symbols is as in Fig. 2.*

We plot in Fig. 4 the $L_X/L_{bol}$ distribution separately for CTTS and WTTS (the average $L_X$ is used for objects observed twice). Because our samples are essentially complete, there is no bias by detection limits. The distributions are close to log-normal, and corresponding Gaussian fits reveal clearly different distributions: WTTS are on average more X-ray luminous (mean of distribution: $\log L_X/L_{bol} = -3.33 \pm 0.07$) than CTTS (mean: $\log L_X/L_{bol} = -3.64 \pm 0.07$), although the widths of the distributions are similar. This finding parallels earlier reports on less complete samples (Stelzer & Neuhäuser, 2001), ruling out detection bias as a cause for this difference. A similar segregation into two X-ray populations has not been identified in most other SFRs (e.g., Preibisch & Zinnecker 2001 - but see recent results on the Orion Nebula Cluster in Preibisch et al. 2005). The cause of the difference seen in TMC may be evolutionary (stellar size, convection zone depth), or related to the presence of accretion disks or the accretion process itself. We will return to this point in Sect. 2.3 below.
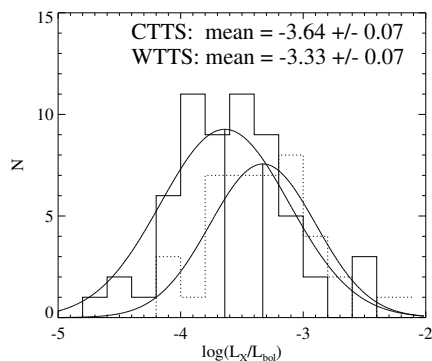


*Figure 4. Comparison of the $L_X/L_{bol}$ distributions for CTTS (solid histogram) and WTTS (dashed), together with log-normal fits. The CTTS sample is on average less luminous (normalized to $L_{bol}$) than the WTTS sample. The errors in the plot indicate the error of the means of the distributions.*

## 2.2. Rotation and Activity

Rotation plays a pivotal role for the production of magnetic fields in main-sequence stars, and thus for the production of ionizing (UV, X-ray) radiation. The rotation rate is controlled by the angular momentum of the young star inherited from the contracting molecular cloud, by the further contraction of the star, but possibly also by torques applied by magnetic fields that connect the star to the circumstellar disk. Strictly speaking, in the standard (solar) $\alpha-\omega$ dynamo theory, it is *differential* rotation that, together with convection, produces magnetic flux near the base of the convection zone. Because the younger T Tau stars are fully convective, a dynamo of this kind is not expected, but alternative dynamo theories based entirely on convective motion have been proposed (e.g., Durney et al. 1993). It is therefore of prime interest to understand the behavior of a well-defined sample of T Tau stars.

In cool main-sequence stars, a rotation-activity relation is found for rotation periods $P$ exceeding a few days (the limit being somewhat dependent on the stellar mass), approximately following $L_X \propto P^{-2.6}$ (Güdel et al., 1997; Flaccomio et al., 2003). Given the role of the convective motion, a better independent variable may be the Rossby number $R = P/\tau$ where $\tau$ is the convective turnover time. If the rotation period is smaller than a few days, the X-ray luminosity saturates at a value of $L_X/L_{bol} \approx 10^{-3}$ and stays at this level down to very short periods.

Previous studies have produced conflicting results on rotation-activity relations. Although there have been indications for such a relation in Taurus (Stelzer & Neuhäuser 2001), samples in other star-forming regions indicate its absence, showing stars at saturated X-ray luminosities all the way to periods of $\approx 20$ days (e.g., Preibisch et al. 2005). There is speculation that these stars are still within the saturation regime because their Rossby number remains small enough for the entire range of $P$, given the long convective turnover times in fully convective stars.

Our complete sample of TTS (for the surveyed area) permits an unbiased investigation of this question with the restriction that we do not know rotation periods for all stars. Rotation periods $P$ are known for 23 TTS (13 CTTS and 10 WTTS) in our sample. Another 23 stars (15 CTTS and 8 WTTS) have measured projected rotational velocities $v \sin i$ which imply upper limits to $P$ once the stellar radius is known. In a statistical sample with random orientation of the rotation axes, the average of $\sin i$ is $\pi/4$ which we used for estimates of $P$ if only $v \sin i$ was known. The stellar radii were calculated from $T_{eff}$ and the (stellar) bolometric luminosity.

The resulting trends are shown in Fig. 5 (here, multiply observed stars are plotted once only, at the average $L_X$ value, see also Briggs et al. 2006). First, it is evident that the sample of CTTS with measured $P$ rotates, on average, less rapidly than WTTS (characteristically, 8 d and 4 d, respectively). Fig. 5a shows that the rotation-activity behavior is clearly different from that of main-sequence solar-mass stars in that $L_X/L_{bol}$ remains at a saturation level up to longer periods. This is not entirely surprising given that the same is true for less massive main-sequence K and M-type stars that are more representative of the TTS sample. Fig. 5b does, however, show a clear trend for decreasing activity with increasing $P$, in particular for periods exceeding $\approx 5$ d. This is best illustrated for the average surface X-ray flux, $F_X = L_X/(4\pi R^2)$.

## 2.3. Accretion and Disks

In the standard dynamo interpretation, the (on average) slower rotation of the CTTS compared to WTTS explains the (on average) slightly lower $L_X$ of CTTS, in analogy to main-sequence stars. The relation suggested above could, however, be mimicked if the CTTS sample, rotating less rapidly, were subject to suppressed X-ray production for another reason than the decreasing efficiency
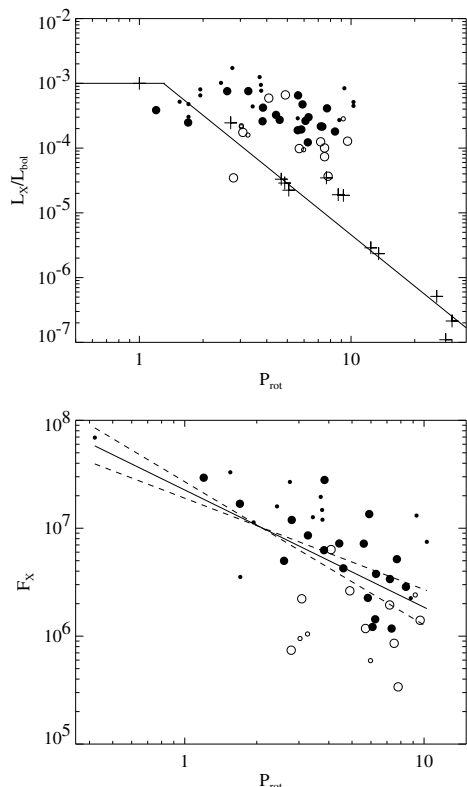
*Figure 5. Rotation properties and rotation-activity relations in the TMC sample.* **Top:** $L_X/L_{\rm bol}$ *for the TMC sample. Symbols are as in Fig. 2. The crosses and the schematic power-law fit resp. horizontal saturation law apply to a sample of solar analogs on the main sequence (Güdel et al., 1997).* **Bottom:** *Same, but for the average surface X-ray flux. Regression fit is also shown.*



*Figure 6. Scatter plots of $L_X$ (top) and $L_X/L_{\rm bol}$ (bottom) versus the mass accretion rates reported in the literature. No trends are evident. Symbols are as in Fig. 2.*

of the rotation-induced dynamo. We already found that the average $L_X/L_{\rm bol}$ is smaller by a factor of two for CTTS compared to WTTS (Sect. 2.2). The most obvious distinction between CTTS and WTTS is accretion from the disk to the star for the former class.

There are at least two arguments against this explanation. First, a rotation-activity relation holds *within* the CTTS sample, and there is no obvious correlation between $P$ and $\dot{M}$ for that sample. And second, when investigating the coronal properties $L_X$, $L_X/L_{\rm bol}$ (and also average coronal temperature $T_{\rm av}$) as a function of the mass accretion rate, we see no trend over three orders of magnitude in $\dot{M}$ (Fig. 6; Audard et al. 2006). Mass accretion rate does therefore not seem to be a sensitive parameter that determines overall X-ray coronal properties.

## 3. JETS AND OUTFLOWS

Shock speeds in the high-velocity component of protostellar jets may be sufficient to shock-heat plasma to X-ray temperatures. The shock temperature is $T \approx 1.5 \times 10^5 v_{100}^2$ K where $v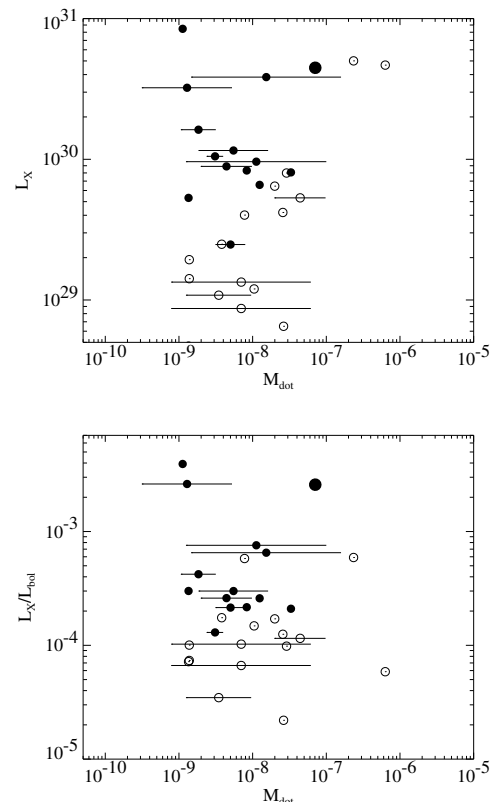_{100}$ is the shock front speed relative to a target, in units of 100 km s$^{-1}$ (Raga et al. 2002). Jet speeds in TMC are typically of order $v = 300 - 400$ km s$^{-1}$ (Eislöffel & Mundt, 1998; Anglada, 1995; Bally et al., 2003), allowing for shock speeds of similar magnitude. If a flow shocks a standing medium at 400 km s$^{-1}$, then $T \approx 2.4$ MK. X-rays have been detected from the L1551 IRS-5 protostellar jet about 0.5–1″ away from the protostar, while the central star is entirely absorbed by molecular gas (Bally et al., 2003).

X-rays of fast flows cannot be traced down to the acceleration or collimation region of protostellar jets given the strong photoelectric absorption in particular of the very soft X-ray photons expected from shocks. An interesting alternative is provided by the study of strong jets driven by optically revealed T Tau stars. Hirth et al. (1997) surveyed TMC CTTS for evidence of outflows and "microjets" on the 1″ scale, identifying low-velocity (tens of km s$^{-1}$) and high-velocity (up to hundreds of km s$^{-1}$) flow components in several of them.

X-ray observations of these jet-driving CTTS have revealed new X-ray spectral phenomenology in at least three, and probably four, of these objects in TMC (DG Tau A - see Audard et al. 2006; GV Tau A, DP Tau - see Fig. 7; and tentatively CW Tau). They share X-ray spectra that are composed of two different emission components subject to entirely different photoelectric absorp-

tion. The soft component, subject to very low absorption ($N_H \approx 10^{21}$ cm$^{-2}$), peaks at 0.7–0.8 keV where Fe XVII produces strong emission lines, suggestive of low temperatures. This is borne out by spectral modeling, indicating temperatures of 2–5 MK. Such temperatures are not common to T Tau X-ray sources. A much harder but strongly absorbed component ($N_H$ several times $10^{22}$ cm$^{-2}$) indicates extremely hot (several tens of MK) plasma.
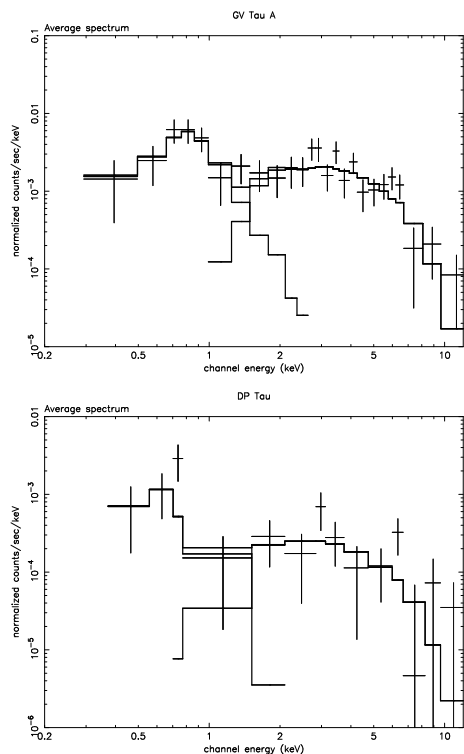


Figure 7. *Average spectra of GV Tau A (top), and DP Tau (bottom). Also shown are the fits to the spectra and their two individual constituents.*

The three definitive examples all show flares in their X-ray light curves (Fig. 8), but such variability is so far seen only in the hard component while the soft component is steady. In the case of DG Tau A and marginally also in GV Tau A, a U-band burst was recorded that precedes the X-ray burst in a characteristic way similar to solar flares (Audard et al., 2006). On the other hand, a comparison with a *Chandra* observation obtained 8 and 6 months before the observation of DG Tau A and GV Tau A, respectively (Güdel et al., 2005) shows at best a small shift in temperature of the soft component with a nearly identical emission measure. Evidently, these "two-absorber" spectra require that *two physically unrelated X-ray sources are present around these objects.*

An obvious model is a binary with components that are located behind largely different gas columns, each thus contributing one of the spectral components. This model is unlikely for the following reasons: i) The less absorbed companion would in all cases reveal a uniquely soft, non-flaring X-ray component only. None of the other TTS in our survey revealed such an X-ray spectrum. ii) Except for GV Tau, the stars with peculiar X-ray spectra
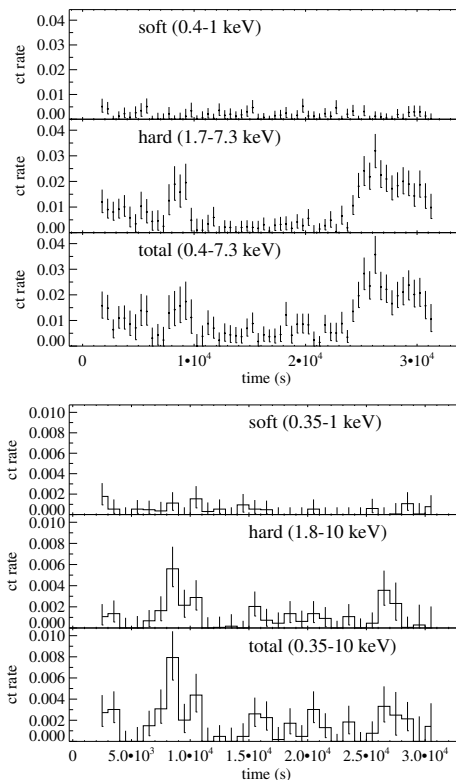


Figure 8. *X-ray light curves of the jet-driving T Tau stars GV Tau A (upper) and DP Tau (lower). The top panels show the soft component, the middle panels the hard component, and the bottom the total X-ray light curves.*

are single, despite detailed searches for components (e.g., Leinert et al. 1991). iii) GV Tau = Haro 6-10 is indeed a binary, the more absorbed component being an embedded protostar behind a large gas column (see Reipurth et al. 2004 for a radio image). A high-resolution *Chandra* image, however, reveals that the soft and hard photons originate from the same location, and this location agrees, within the error ranges for *Chandra*, the VLA (Reipurth et al. 2004) and 2MASS, with the less absorbed component Haro 6-10A (Güdel et al. 2006, Fig. 9).



Figure 9. *Chandra images of the region around the GV Tau = Haro 6-10 binary. Pixel size is 0.5″.* **Left:** *Soft band, 0.5–1 keV;* **Right:** *Hard band, 2.2–7 keV. The two crosses indicate the positions of Haro 6-10A (south) and the deeply embedded protostar Haro 6-10B (north). The separation between the two components is 1.3″.*

All these stars are strong accretors ($\dot{M}$ of order $10^{-7}$ to $10^{-6}$ M$_\odot$ yr$^{-1}$). However, as shown above, the TMC sample reveals no significant relation between mass accretion rate and coronal properties. The distinguishing property of these objects is, in contrast, the presence of well-developed, protostar-like jets and outflows with appreciable mass-loss rates ($10^{-7}$ to $10^{-6}$ M$_\odot$ yr$^{-1}$).

A tentative interpretation is the following (Güdel et al., 2005, 2006): The flaring in the hard component occurs on timescales of hours, suggesting ordinary coronal active regions. The preceding U-band bursts signal the initial chromospheric heating before plasma is evaporated into the magnetic loops. The flaring active regions are therefore likely to be of modest size, well connected to the surface active regions. The excess absorption is probably due to cool gas that streams in from the disk along the magnetic field lines, enshrouding the magnetosphere with absorbing material. This increases the photoelectric absorption of X-rays but does not increase optical extinction because the gas streams are very likely to be depleted of dust (the latter being evaporated farther away from the star). As for the cool X-ray component, although its temperature is also compatible with shock heating of material in accretion columns close to the star (e.g., Kastner et al. 2002), the low photoabsorption makes this interpretation problematic and prefers a location outside the magnetosphere. An obvious location of the cool, soft X-ray sources are shocks forming near the base or the collimation region of the jet (e.g., Bally et al. 2003). Jet speeds of several hundred km s$^{-1}$ support this model, as do estimated X-ray luminosities (see Güdel et al. 2005, based on the theory of Raga et al. 2002).

If this model is correct, then the consequences are far-reaching: distributed, large-scale X-ray sources may efficiently ionize larger parts of the circumstellar environment than the central star alone, and in particular the disk surface, thus inducing disk accretion instabilities (Balbus & Hawley, 1991) and altering the disk chemistry (Feigelson & Montmerle, 1999; Glassgold et al., 2004).

## ACKNOWLEDGMENTS

## REFERENCES

van den Ancker M. E., et al. 1997, A&A, 324, L33

Anglada G. 1995, RevMexAA, 1, 67

Audard M., et al. 2006, this volume

Balbus S. A., & Hawley J. F. 1991, ApJ, 376, 214

Bally J., Feigelson E., & Reipurth B. 2003, ApJ, 584, 843

Bouvier J. 1990, AJ, 99, 946

Briggs K. R., et al. 2006, this volume

Damiani F., & Micela G. 1995, ApJ, 446, 341

Damiani F., Micela G., Sciortino S., & Harnden F. R. Jr. 1995, ApJ, 446, 331

Durney B. R., De Young D. S., & Roxburgh I. W. 1993, Sol. Phys., 145, 207

Eislöffel J., & Mundt R. 1998, AJ, 115, 1554

Feigelson E. D., & Montmerle T. 1999, ARA&A, 37, 363

Feigelson E. D., Jackson J. M., Mathieu R. D., Myers P. C., & Walter F. M. 1987, AJ, 94, 1251

Flaccomio E., Micela G., & Sciortino S. 2003, A&A, 402, 277

Glassgold A. E., Najita J., & Igea J. 2004, ApJ, 615, 972

Grosso N., et al. 2006, this volume

Güdel M., Guinan E. D., & Skinner S. L. 1997, ApJ, 483, 947

Güdel M., et al. 2005, ApJ, 626, L53

Güdel M., et al. 2006, A&A, in prep.

Hirth G. A., Mundt R., & Solf J. 1997, A&AS, 126, 437

Kastner J. H., Huenemoerder D. P., Schulz N. S., Canizares C. R., & Weintraub D. A. 2002, ApJ, 567, 434

Leinert Ch., Haas M., Mundt R., Richichi A., & Zinnecker H. 1991, A&A, 250, 407

Neuhäuser R., Sterzik M. F., Schmitt J. H. M. M., Wichmann R., & Krautter J. 1995, A&A, 297, 391

Preibisch T., & Zinnecker H. 2001, AJ, 122, 866

Preibisch T., et al. 2005, ApJS, 160, 401

Raga A. C., Noriega-Crespo A., & Velázquez P. F. 2002, ApJ, 576, L149

Reipurth B., Rodríguez L. F., Anglada G., & Bally J. 2004, AJ, 127, 1736

Stelzer B., & Neuhäuser R. 2001, A&A, 377, 538

Strom K. M., & Strom S. E. 1994, ApJ, 424, 237

Strom, K. M., et al. 1990, ApJ, 362, 168

Walter F. M., Brown A., Mathieu R. D., Myers P. C., & Vrba F. J. 1988, AJ, 96, 297